ELSEVIER

NeuroImage

www.elsevier.com/locate/ynimg
NeuroImage 23 (2004) 1059–1067

Hunting for neuronal currents: absence of rapid MRI signal changes during visual-evoked response

Renxin Chu,[a] Jacco A. de Zwart,[a] Peter van Gelderen,[a] Masaki Fukunaga,[a] Peter Kellman,[b] Tom Holroyd,[c] and Jeff H. Duyn[a,*]

[a]*Advanced MRI Section, LMFI, NINDS, National Institutes of Health, Bethesda, MD, United States*
[b]*Laboratory of Cardiac Energetics, NHLBI, National Institutes of Health, Bethesda, MD, United States*
[c]*MEG Facility, NIMH, National Institutes of Health, Bethesda, MD, United States*

Received 17 February 2004; revised 1 June 2004; accepted 2 July 2004
Available online 28 September 2004

While recent reports have advocated the use of magnetic resonance imaging (MRI) to detect the effects of neuronal currents associated with human brain activity, only preliminary experimental data have been presented so far to demonstrate the feasibility of the method. Furthermore, it has not been adequately demonstrated that (1) MRI can separate neuronal current (NC) effects from other effects such as blood oxygen level-dependent (BOLD) contrast; (2) MRI has adequate sensitivity to detect NCs in vivo. In this work, we introduce a method that can separate slow (e.g., BOLD) processes from potential rapid (e.g., NC) processes and apply this method to investigate whether MRI allows detection of an NC response to a visual stimulus. MRI studies ($n = 8$) at 3.0 T using a sensitive multichannel detector showed insignificant effects related to NCs (averaged $t < 0.05$), in the presence of a highly significant BOLD signal ($t = 6.15 \pm 0.90$). In contrast, magnetoencephalography (MEG) experiments performed under similar conditions on the same subjects showed highly significant electrical activity ($t = 7.90 \pm 2.28$). It is concluded that, under the conditions used in this study, the sensitivity of MRI to detect evoked responses through NCs is at least an order of magnitude below that of BOLD-based functional MRI (fMRI) or MEG and too low to be practically useful.
Published by Elsevier Inc.

Keywords: Neuronal currents; Magnetoencephalography; Human brain

Introduction

Both spatial and temporal resolution of blood oxygen level-dependent (BOLD) functional magnetic resonance imaging (fMRI) are limited by the underlying physiologic processes, including the dilation of the arteriolar vasculature through neurovascular coupling (Zonta et al., 2003), the ensuing flow response (Kwong et al., 1992), and the hemoglobin transit through the capillary bed and macrovasculature (Duyn et al., 1994; Lee et al., 1995; Mandeville and Marota, 1999). The temporal resolution of fMRI and maybe also its spatial resolution could be substantially improved if MRI can be sensitized to detect the changes in electrical activity associated with brain activation. Changes in both microscopic (e.g., neuronal spiking) and macroscopic electrical activity (e.g., local field potentials) occur on time scales well below the BOLD time scale of several seconds and contain potentially important information, complementary to that available through the BOLD-based signals. On the other hand, established techniques that measure electrical brain activity through intracranial electrodes, voltage sensitive dyes (Shoham and Grinvald, 2001), or electroencephalography (EEG) and magnetoencephalography (MEG) are either invasive or have poor spatial resolution.

Recently, a number of researchers have suggested the use of fMRI to detect changes in neuronal currents (NCs) during human brain activation (Bodurka and Bandettini, 2002; Kamei et al., 1999; Konn et al., 2003; Xiong et al., 2003). One of the claims is that NC-based MRI has the ability to detect visual and sensorimotor activation with a sensitivity similar to that of BOLD fMRI (Xiong et al., 2003). However, as of yet, this claim has not been validated. Furthermore, previously proposed methodology (Xiong et al., 2003) has a relatively poor efficiency at detecting NCs and does not optimally separate NC contrast from BOLD contrast.

The purpose of the current work was to design an fMRI method that is highly sensitive to both the rapid and slow effects associated with NC and BOLD contrast, respectively, while at the same time allowing for excellent separation of the two effects. Furthermore, the new method was used to quantify the relative sensitivities of NC and BOLD contrast in fMRI experiments of the human visual system and to compare these with the sensitivity of MEG.

* Corresponding author. Advanced MRI Section, LFMI, NINDS, National Institutes of Health, Building 10, Room B1D-118, 9000 Rockville Pike. Bethesda, MD 20892-1065. Fax: +1 301 480 2558.
E-mail address: jhd@helix.nih.gov (J.H. Duyn).
Available online on ScienceDirect (www.sciencedirect.com.)

1053-8119/$ - see front matter. Published by Elsevier Inc.
doi:10.1016/j.neuroimage.2004.07.003

Materials and methods

Experimental design

The fMRI method was designed to measure BOLD effects and potential NC effects simultaneously, separably, and with high sensitivity. MRI contrast to NCs was envisioned to originate from the effects of intracellular dendritic currents on the MRI signal, including signal amplitude (magnitude) reduction due to intravoxel dephasing (Xiong et al., 2003) and possibly signal phase effects (Kamei et al., 1999). To optimally capture these signal changes, single shot gradient echo EPI was performed with long (81 ms) TE (Xiong et al., 2003), which is on the time scale of the evoked responses measured by EEG and MEG. To further improve sensitivity, a short TR (100 ms) was used in combination with a high stimulation rate (see below). To maintain adequate image signal-to-noise ratio (SNR) under the saturating conditions resulting from TR = 100 ms, SNR was boosted by performing the experiments at 3.0 T using a 16-channel brain coil (de Zwart et al., 2004) connected to a 16-channel receiver (Bodurka et al., 2004), both developed in collaboration with Nova Medical Inc. (Wakefield, MA, USA).

Stimulation protocol

The activation studies were performed in the human visual system, known for its robust BOLD fMRI and MEG/EEG responses. To allow separation of the (slow) BOLD effects from potential (fast) NC effects, a dedicated stimulation protocol was used based on the binary m-sequence probe method (Kellman et al., 2003; Sutter, 2001). The binary m-sequence probe method allows efficient determination of linear and nonlinear aspects of the fMRI impulse response (Buracas and Boynton, 2002; Kellman et al., 2003). The protocol (Fig. 1) consisted of a combination of two pseudorandom m-sequences: a rapid sequence consisting of 20 bins, each with a duration (base period) of 100 ms (equal to the MRI TR), and a slow sequence with 150 bins, each with a base period of 2000 ms. The idea was to use the slow m-sequence to extract a "coarse" BOLD impulse response (IR) and the rapid m-sequence to extract a "fine" NC IR. The rapid 20-bin sequence consisted of a 15-bin m-sequence and five additional bins (repeat of the first five bins), whereas the 150-bin slow sequence consisted of a 127-bin m-sequence, and 23 additional bins. The extra bins were inserted to avoid unwanted transient effects, such as the initial signal drop related to the approach to NMR steady state.

Each m-sequence contained a close to equal number of "0" and "1" values. Rapid m-sequence bins with values "1" corresponded to visual presentation of a circular checkerboard pattern of 50-ms duration, followed by 50 ms of darkness, while bin values "0" corresponded to 100-ms darkness. The slow sequence was used in a modulatory fashion: during bin values "1" in the slow m-sequence, the rapid m-sequence was played out (2000 ms), while no stimulus was presented for 2000 ms during bin values "0". A total of 3000 (150 × 20) m-sequence bins were played out, of which 25% represented an active (checkerboard) stimulus.

The stimulus was back-projected using a DLP projector (U2 1200, Plus Corp., Tokyo, Japan) on a translucent screen, just behind the subject's head, and viewed via a mirror. The check size of the checkerboard pattern was scaled with eccentricity, in an attempt to maintain a constant (strong) stimulation across the primary visual cortex (Horton and Hoyt, 1991). The luminance of white squares varied from 120–250 Cd/m^2, the visual angle of the stimulus (radius) varied from 10° to 15°. The luminance of the checkerboard stimulus was modulated over time (using the m-sequence protocol described above) using a computer-controlled, ferroelectric liquid-crystal shutter (LV4500P-OEM, Displaytech

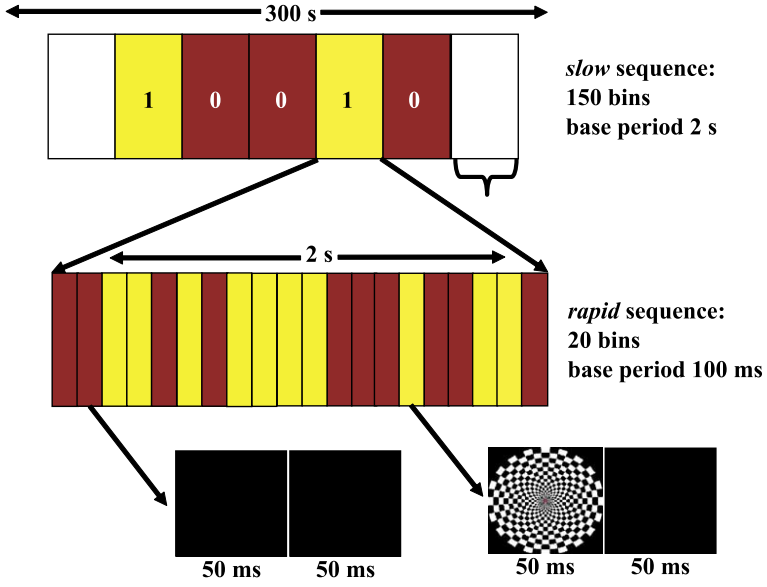

Fig. 1. The modulated binary m-sequence used to simultaneously map slow (BOLD) and fast (NC) responses. An m-sequence with a base period of 2 s (slow m-sequence) was used to generate a slow stimulus variation to elicit BOLD signals. During m-sequence zeroes (red bins), no visual stimulus was presented. During m-sequence ones (yellow bins), a second m-sequence was played out at rapid pace (100-ms base period) to allow measurement of fast signal responses. During fast m-sequence ones (yellow bins), a checkerboard visual stimulus was presented (50-ms checkerboard, followed by 50-ms darkness), whereas during fast m-sequence zeroes (red bins), no stimulus (darkness) was presented for 100 ms.

Inc, Longmont, CO, USA) with a transition time of 70 μs. Shutter switching was controlled from a programmable trigger line in the MRI pulse sequence and synchronized to the MRI excitation pulse at the start of each TR.

MRI data acquisition

Functional MRI studies were performed on eight normal volunteers on a General Electric 3-T scanner, using a home-written gradient-echo EPI sequence (Kellman et al., 2003). A single, axial-oblique slice of 5-mm thickness, centered on the calcarine fissure was scanned with 3.4 × 3.4 mm^2 nominal in-plane resolution and 220 × 165 mm^2 field of view. The EPI readout bandwidth was 250 kHz, and the total echo train duration was 24 ms. A 25° excitation flip angle was used, which resulted in minimal image contrast (beneficial for temporal stability) and provided good image SNR, as it was close to the Ernst angle of 21° for cortical grey matter (T1 = 1500 ms). RF phase scrambling was performed using 45° phase increment to improve temporal stability and reduce the contribution of stimulated echoes. The latter would potentially have introduced undesirable temporal blurring due to spillover of magnetization into subsequent TR intervals. Although quadratic RF phase scrambling does not completely eliminate stimulated echoes, it can suppress them quite effectively, even in the presence of pulsations and motion (Duyn, 1997). An extra central k-space line was acquired to reduce EPI ghosting (Bruder et al., 1992). On seven of the eight subjects, the MRI phase was measured before the EPI readout to allow derivation of phase images with correction for large-scale temporal phase fluctuations. Linear shims were adjusted before the functional scans to optimize the signal strength in occipital areas at TE = 81 ms.

High-resolution T1-weighted images were obtained to allow mapping of the MRI and MEG functional data on an anatomical reference. For this purpose, the product inversion recovery 3D FSPGR sequence was used with the following parameters: TE = 3.2 ms, TR = 7.9 ms, TI = 300 ms, flip angle = 17°, 1 × 1 mm^2 in-plane resolution, and 1–2 mm through-plane resolution. This MP-RAGE-like (Mugler and Brookeman, 1990) sequence provides efficient acquisition of images with good contrast between grey and white matter. On each subject, two to four experimental runs were performed. Two different delays (0 and 50 ms) between the stimulus sequence and the fMRI acquisition were investigated, in anticipation of a potential cancellation of the NC IR due the often multiphasic nature of the electrical signals (see below).

Before each scan session, normal volunteers (four males and four females, aged 22.5–55.9 years, 32.3 years average) gave written, informed consent to participate in the study, which was approved by the Intramural Review Board (IRB) at the National Institutes of Health under protocol number 00-N-0082. For the MRI studies, earplugs were provided for hearing protection because of the excessive acoustic noise generated by the gradient system.

MEG data acquisition

MEG was performed with the same stimulus protocol on the same eight subjects as used for the MRI experiments using a 275-channel gradiometer system (Omega 2000, VSM Medtech Ltd., Canada). For the MEG studies, the stimulus was back-projected using an LCD projector (Notevision XG-P10XU, Sharp Inc, USA) with a luminance and visual angle similar to that of the MRI setup. MEG data were acquired at 600 Hz and down-sampled to 150 Hz. The timing of the stimulus, controlled from a programmable arbitrary waveform generator (33250A, Agilent Technologies Inc, USA), was recorded with the MEG data by measuring the light output timing from a photodiode sensor placed in the projector beam outside the focal plane. On each subject, two to four experimental runs were performed.

Data analysis

MRI and MEG data were analyzed in similar fashion using correlation analysis (Kellman et al., 2003). MRI data were analyzed for signal intensity (magnitude) and phase effects. Before correlation analysis, both MEG and MRI data were high-pass filtered with a cutoff at 0.005 Hz, and the MEG data were notch-filtered at 60 and 120 Hz to remove line interference. Furthermore, on the MRI data, spectral frequencies related to cardiac and pulmonary cycles were identified and removed using digital filtering before correlation analysis. Two to four spectral frequencies were removed using Gaussian-shaped stop bands each with a full width at half maximum of 0.2 Hz.

For the MRI data, channel-combination and image reconstruction was performed as described previously (de Zwart et al., 2002, 2004). This allowed reconstruction of phase and magnitude data. To avoid phase wrapping, the average phase of the time-series data was subtracted from each time point. Large-scale phase fluctuations related to subject motion or hardware instabilities were corrected using the phase measurement preceding the EPI acquisition. From the time-series data, fMRI activation signals were extracted by correlating with a 20-fold zero-filled version of the slow m-sequence (Fig. 2). Only the

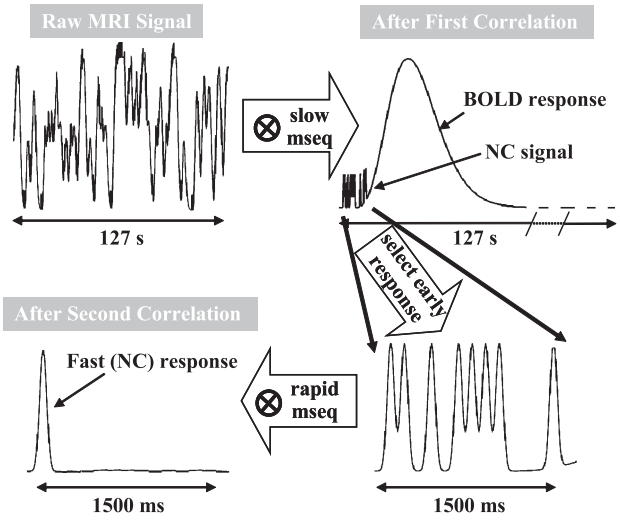

Fig. 2. Extraction of BOLD and NC responses. Two sequential correlation analyses are performed. During the initial analysis, a 127-s segment of the MRI intensity (or phase) time-course is correlated against the slow m-sequence. The resulting signal is the estimated "coarse" IR to a 2000-ms (rapid m-sequence) stimulus, including BOLD signals and NC signals. In a second analysis step, the early part of the "coarse" IR is correlated against the rapid m-sequence. The resulting signal contains the "fine" NC IR to a single 50-ms checkerboard presentation.

linear kernel (h_1, see Kellman et al., 2003) was used. The resulting signal contains the "coarse" IR to a 2000-ms rapid m-sequence stimulus, including potential NC signals in the first part of the response (0 to approximately 2200 ms), and a delayed BOLD signal in the later part of the response. The "fine" IR to the 50-ms checkerboard stimulus (related to NC and other fast effects) was extracted by subsequent correlation of the early part of the response (obtained after the initial correlation) with the rapid m-sequence. For this purpose, the first two bins of the "coarse" IR were skipped, and only bins 3–17 were used to avoid any transient effects from preceding rapid m-sequence segments. Note that these bins contain information similar (except for the noted transient effects) to that contained in bins 2–16 or 1–15. Due to the high-pass temporal filtering inherent to this correlation analysis and the low amplitude of the BOLD response in this early time segment, this resulted in a signal selectively sensitive to rapid processes correlated with the m-sequence stimulus (e.g., NC effects) and suppression of the (slow) BOLD signal. For convenience, from now on, we will refer to the delayed signal extracted after initial correlation with the slow m-sequence as "BOLD IR" and the fast signal extracted after secondary correlation with the rapid m-sequence as "NC IR."

For the MEG data, a similar analysis was performed, with the exception that correlation was not performed with the numerical m-sequence, but rather with the recorded photodiode signal. After correlation, synthetic aperture magnetometry (SAM) (Robinson and Virba, 2002) was used to determine coarse spatial location relative to a separately recorded T1-weighted MRI.

Statistical analysis was performed by normalizing correlation amplitudes to the temporal noise levels. The temporal noise level was determined from the temporal standard deviation (TSD) as calculated from response-free segments of the correlogram (Kellman et al., 2003). For the TSD of the BOLD IR (TSD–BOLD), this was done after 20-fold down-sampling (to 2-s bins) of the correlogram obtained after correlation with the slow m-sequence. The TSD of the NC IR (TSD–NC) was obtained from subsequent correlation of BOLD-free data (lag > 30 s) with the rapid m-sequence. Activated pixels in the visual cortex were selected by thresholding ($t = 3.5$) the BOLD IR in the time interval (correlation lag) 2–6 s. Using these pixels, average t score of the BOLD response and average t score of the NC IR were calculated. In addition, t scores were determined on region of interest (ROI) averaged correlation signals, normalized to the TSD of the ROI-averaged signal. This analysis is equivalent to the use of general linear model (GLM) analysis with multiple delayed delta functions as explanatory variables to account for the BOLD and NC responses.

Furthermore, to evaluate temporal signal stability of the MRI method, the relative TSD (in % of the baseline signal) was determined from the image intensity time course on a pixel-by-pixel basis. In addition, to obtain a stability measure not limited by image SNR, TSD was determined on the signal average of all activated pixels (TSD–ROI). This was done after temporal high-pass filtering with a cutoff at 0.33 Hz to remove slow signal fluctuations, including BOLD effects. All TSD values were calculated as a percentage of baseline image intensity.

For the MEG data, t scores were calculated per sensor, after which an average absolute t score was determined for all sensors from a group (out of 42 occipital sensors) with absolute t values exceeding 3.5 in a time interval 80–130 ms following impulse (50-ms checkerboard display) onset.

Results

Image quality

The raw EPI–MRI images were somewhat affected by signal dropout due to intravoxel dephasing, as expected under the conditions of long TE (81 ms), high magnetic field (3.0 T) and large voxel size. However, image quality was reasonable in occipital areas, partly because of the manual shim optimization before scanning. In all subjects, the SNR exceeded 30:1 in the visual cortex, and the TSD averaged 2.87% (Table 1). The TSD of the average signal in the activated pixels (TSD–ROI) was 0.49%, which was far below the single-pixel TSD. This suggests that the scan method was highly stable and furthermore that the pixel-based TSD was limited by the image SNR.

BOLD signal

Two of the functional runs were discarded due to problems with the stimulus presentation (from subjects 1 and 2, see Table 1). In all remaining runs, significant BOLD IRs were observed. Across subjects, the maximum ROI-averaged t score (t-slow) ranged from 3.83 to 7.48 (Table 1). The t score of the ROI-averaged "coarse" IR was 16.6 ($\pm$4.0). The ROI-averaged BOLD signal amplitude, as a percentage of baseline signal, ranged from 1.3% to 2.4%. No significant difference was found between the runs with different delays (results not shown). Fig. 3 shows the IR obtained after correlation with the slow m-sequence, averaged over all activated pixels (and all subjects). The BOLD IR resembled a gamma-variate function and reached a maximum of 1.53% ($\pm$0.39%) of the baseline signal at around $t = 4.5$ s. The curve was relatively flat in the 0- to 2-s interval, where it had a noise-like appearance. Its average correlation signal amplitude in this interval was only a small fraction (<3%) of the average BOLD level in the 2- to 8-s interval. This is suggestive of an absence of NC effects (see below).

NC signal

No significant correlation with the rapid m-sequence was found in the visual cortex (active BOLD pixels) in either MRI signal magnitude or phase in any of the MRI runs, both for single pixels as well as for the ROI averaged signal, and for both the 0-ms and the 50-ms delay between stimulus and data acquisition (see MRI data acquisition) runs. This suggests an absence of fast (NC) effects in the MRI data. The average signal level of the NC IR was below 0.2% of the baseline signal in all subjects. The t score of the NC IR, averaged over the pixels with significant BOLD activation (see above), was below 0.6 at all correlation lags. At the 0th and 1st correlation lag (IR between 0–100 ms and 100–200 ms, respectively), covering the time period of maximal MEG-IR, the absolute value of the t score was below 0.47 in all subjects (Table 1).

An example of the results in a single subject is given in Fig. 4. Most of the BOLD activity mapped to the visual areas in the occipital lobe (Fig. 4a). The time course of the ROI-averaged t score, obtained from correlation with the slow m-sequence (Fig. 4b, black curve), showed a highly significant BOLD IR ($t > 7$), and a noise-like early response (Fig. 4b, inset). The response remained at noise level after correlation with the second (rapid)

Table 1
Overview of MRI and MEG experiments on eight subjects

Subject	MRI data									MEG data	
	Delay (ms)	TSD (%)	TSD–ROI (%)	No. of active voxels	BOLD *t*-slow (SD)	NC *t*-fast 0–100 ms		NC *t*-fast 100–200 ms		No. of active sensors	*t*-MEG
						Mag.	Phase	Mag.	Phase		
1	0	3.91	0.95	43	3.83(0.45)	−0.36	–	0.05	–	9; 17	6.27; 6.97;
2	0	3.96	0.68	84	4.58(0.75)	−0.19	0.03	0.05	−0.12	21; 21	5.42; 6.05;
3	0	4.39	0.55	117	7.48(1.50)	−0.03	−0.13	0.01	−0.18	12; 4; 18	4.69; 5.24;
3	0	4.51	0.64	106	7.40(1.41)	0.05	0.13	0.03	−0.36		4.90
3	50	3.71	0.53	101	5.20(0.95)	−0.09	0.03	0.07	−0.14		
3	50	3.48	0.50	149	6.20(1.41)	−0.07	−0.03	−0.16	0.14		
4	50	2.99	0.43	105	7.05(1.34)	0.04	−0.02	0.12	0.06	30; 33; 37	8.86; 10.69;
4	0	3.52	0.41	114	6.85(1.36)	−0.03	−0.09	0.13	−0.11		10.73;
4	50	3.14	0.34	164	6.81(1.63)	0.01	0.00	−0.04	−0.14		
4	0	3.12	0.45	142	6.55(1.44)	−0.01	0.09	0.01	0.04		
5	0	2.85	0.31	110	6.96(1.36)	−0.04	0.06	−0.10	0.22	10; 12; 27	6.55; 6.73;
5	50	2.27	0.34	85	6.46(1.11)	−0.02	0.12	0.04	−0.06		6.41
6	50	2.77	0.58	62	6.15(0.90)	0.17	0.17	−0.03	−0.05	22; 23; 18	6.42; 7.00;
6	0	2.94	0.52	68	5.60(0.86)	0.04	0.00	0.19	0.04		5.89
6	0	2.89	0.42	86	5.53(0.94)	0.13	0.10	0.14	0.10		
6	50	3.67	0.56	78	6.70(1.10)	−0.03	0.11	−0.07	−0.12		
7	50	1.59	0.45	102	6.13(1.13)	0.07	0.26	0.07	−0.21	33; 34; 27;	10.06; 8.24;
7	0	1.57	0.45	84	5.36(0.89)	0.00	0.25	0.01	0.47	28;	9.59; 8.62
7	50	1.66	0.48	72	5.49(0.85)	0.12	−0.12	0.24	0.04		
7	0	1.54	0.45	96	5.19(0.79)	−0.10	−0.32	−0.18	0.31		
8	0	2.21	0.37	135	6.51(1.40)	−0.08	0.20	−0.03	0.22	26; 28; 20;	10.62; 11.81;
8	50	2.02	0.45	110	7.06(1.37)	0.20	0.08	0.15	0.35	17	10.05; 11.79
8	0	2.03	0.41	126	6.19(1.27)	−0.18	−0.14	0.05	−0.15		
8	50	2.16	0.43	102	6.41(1.18)	−0.09	−0.05	0.01	0.02		
Average	–	2.87	0.49	100.5	6.15(1.14)	−0.02	0.03	0.02	0.03	22.4	7.90
SD	1.4	0.91	0.14	29.3	0.90(0.29)	0.12	0.16	0.11	0.20	8.0	2.28

BOLD *t* scores (*t*-slow) are compared with NC *t* scores at the first (*t*-fast, 0–100 ms) and second (*t*-fast, 100–200 ms) correlation lags, and with the MEG *t* score (*t*-MEG). For the NC signal, both magnitude (Mag.) and phase effects are shown. MRI *t* scores are averages over active ROI; MEG *t* scores are averages over active sensors. TSD indicates the average single voxel TSD; TSD–ROI is the TSD of signal averaged over active ROI; "Delay" indicates the time shift between stimulus and acquisition (see MRI data acquisition); MEG data for different runs are separated by semicolons.

m-sequence (Fig. 4b, red curve). The t maps of the individual runs showed noise-like patterns without distinct features of apparent functional significance. Only the phase data occasionally contained one or two pixels exceeding the *t* threshold; however, these were always outside the visual cortex. An example of t maps of individual runs is shown in Fig. 4c for the first eight correlation lags. Phase and magnitude analysis is shown for runs with both 0- and 50-ms delay.

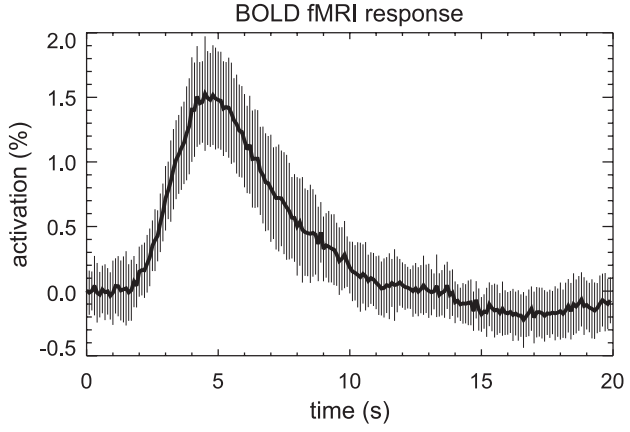

Fig. 3. Magnitude BOLD fMRI response obtained from correlation with the slow m-sequence, as percentage of baseline signal, and averaged over all activated pixels in all runs (all subjects). The vertical bars indicate the standard deviation of the ROI-averaged response across subjects. While a strong BOLD IR is observed after $t = 2$ s, low BOLD levels occur in the preceding period, used for extraction of the fast (NC) response.

Fig. 5 shows, for each of the MRI runs, the temporal characteristics of the ROI-averaged signal magnitude (Fig. 5a) and phase (Fig. 5b) after correlation with the rapid m-sequence and normalized to ROI-averaged temporal noise levels (see Materials and methods). The NC IRs have a noise-like character, with no significant departure from noise level at any correlation lag ($t < 3$, $P = 0.0026$), again suggesting the absence of NC effects.

MEG signal

After correlation with the slow and rapid m-sequence, all of the MEG runs also showed significant activation, as determined from the early part of the first order (linear) IR. The largest activity was observed in occipital sensor locations with sensor-averaged *t* scores ranging from 4.69 to 11.81 (Table 1). SAM analysis showed that most of the activity mapped to visual areas. An example is shown in Fig. 6a, where SAM activity was projected onto a surface-rendered MRI of grey matter anatomy, as well as overlain

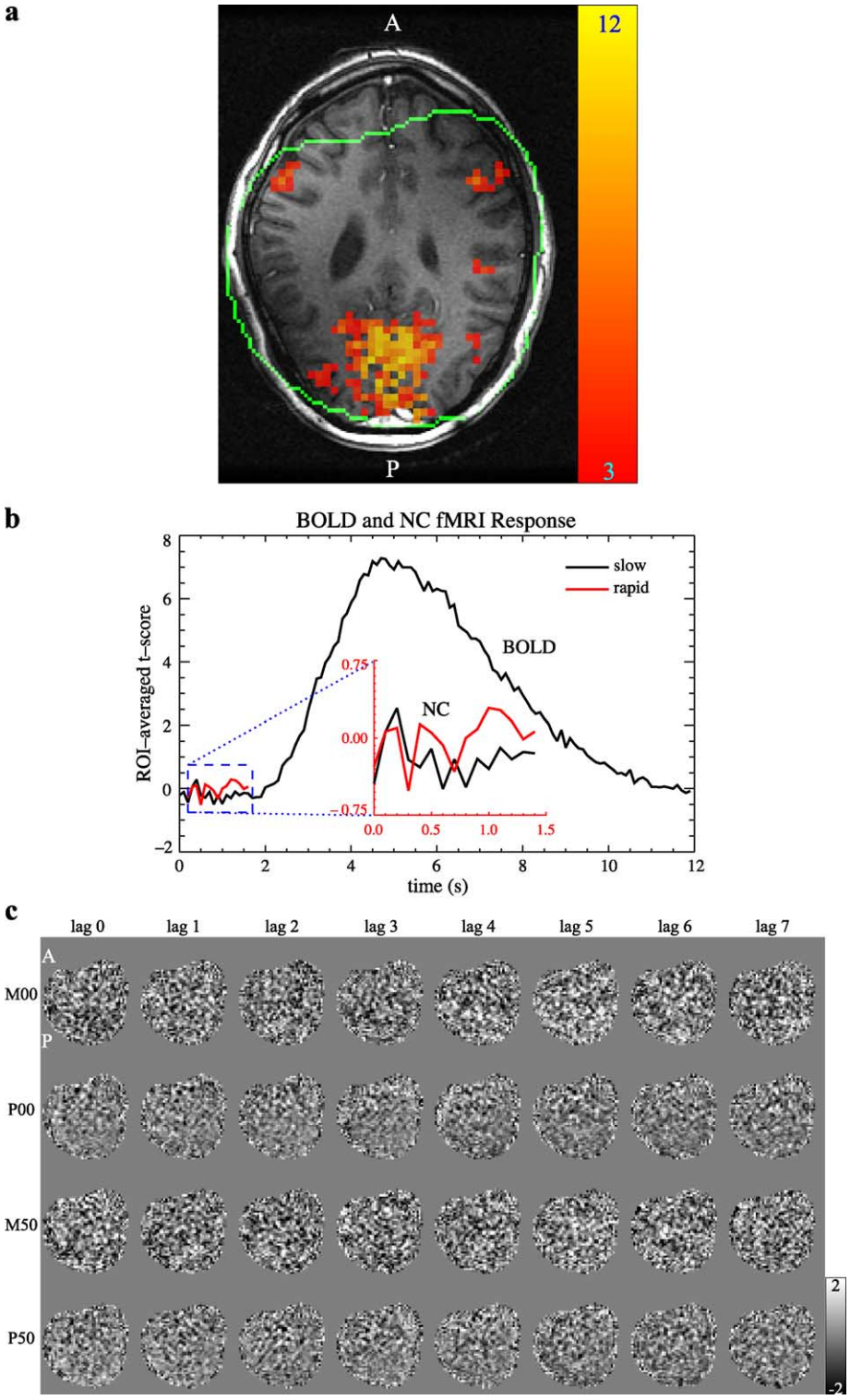

Fig. 4. Example of the fMRI results as measured by the dual m-sequence method. Shown are averages of three runs on a single subject. Anterior (A) and posterior (P) anatomical locations are indicated were applicable. (a) BOLD t map overlain on a T_1-weighted high-resolution anatomical scan. The range of t values is indicated on the scale bar on the right. A strong BOLD signal is present in the occipital cortex. The outline of the area covered by the functional data is indicated by the green line. (b) BOLD and NC IR after correlation with slow (black) and rapid (red) m-sequence. ROI-averaged t scores suggest a highly significant BOLD signal. The inset shows an expansion of the 1500-ms interval used for extraction of NC IR, suggesting an absence of any significant signals. (c) MRI–NC response in brain slice displayed in (a) for magnitude analysis and 0-ms delay (M00); phase analysis, 0-ms delay (P00); magnitude analysis, 50-ms delay (M50); and phase analysis, 50-ms delay (P50). The first eight time points of the IR are shown, each representing a 100-ms timeframe. Note the virtual absence of any image features other than random-appearing noise.

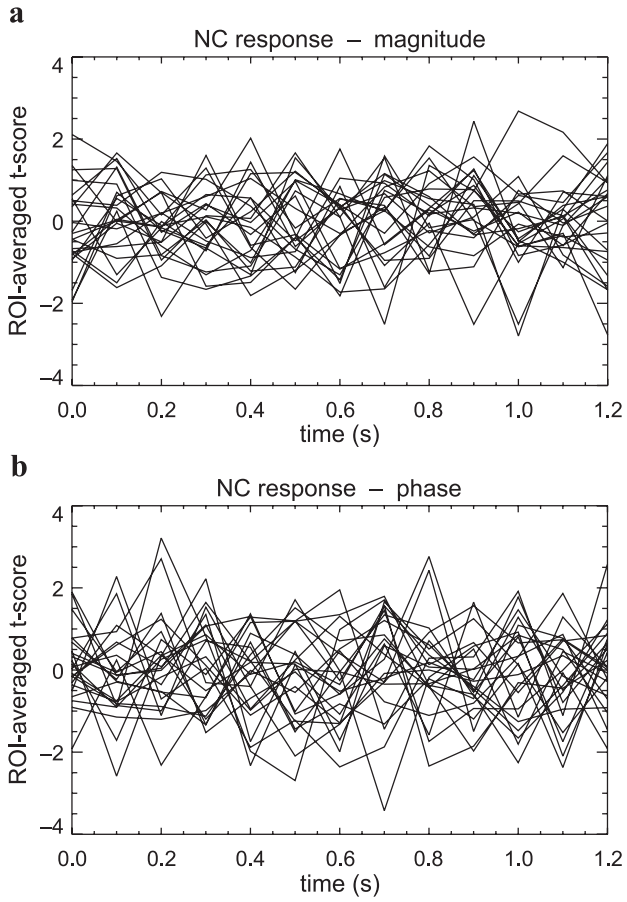

Fig. 5. NC response for each of the MRI runs using magnitude (a) and phase (b) analysis. The response was calculated from the magnitude of the ROI-averaged correlation signal, normalized to TSD–NC of the ROI-averaged signal (see Data analysis). The absence of any significant NC response is evident.

on an axial-oblique slice of the T1-weighted localizers (same subject and similar slice location as for Fig. 4). A comparison of MEG and fMRI-based NC signals in the same subject is shown in Fig. 6b. Single-sensor t scores (combined data from three runs) showed values exceeding 20 in the first 200 ms of the IR (Fig. 6b), while average MRI NC t score in the active ROI was below 0.4.

Discussion

General remarks

A novel technique was developed that allows separation of fast and slow signals in response to neuronal activation. The technique was combined with a sensitive MRI scan technique to investigate the feasibility to detect evoked electrical activity in the human visual system. In contrast with previous reports (Kamei et al., 1999; Xiong et al., 2003), evoked NCs did not lead to significant rapid signal changes in MRI, while slow (BOLD) signal changes were highly significant. Furthermore, in separate experiments performed on the same volunteers, rapid signals measured with MEG were highly significant. This suggests that, while our stimulus protocol is effective in generating NCs, the effects of these NCs on the MRI signal are too small to be measured above the noise level.

fMRI sensitivity

When assuming that earlier studies (Kamei et al., 1999; Xiong et al., 2003) truly observed NC effect, the failure of detecting NC effects with the current MRI methodology is surprising, given its superior sensitivity. In the following, we will look at the relative sensitivity of our method in more detail.

In general, the sensitivity of an fMRI method is augmented by (1) increasing the activation-related signal change, (2) minimizing the TSD, and (3) increasing the number of averages:

(1) The signal change related to neuronal current effects is dependent on the TE of the MRI acquisition, as well as the underlying contrast mechanism. Despite the uncertainties with details of the NC contrast mechanism, one would expect a similar TE dependence as with MRI methods based on microscopic susceptibility contrast agents (Menon et al., 1993; Weisskoff et al., 1994; Yablonskiy and Haacke, 1994), which suggest an exponential signal decay, and therefore the percentage signal change that has a close to linear dependence on echo time. This is in contrast with the quadratic relationship observed by Xiong et al. (2003). Assuming that the percentage TSD is independent of TE, the optimal choice of TE would be close to the time scale of the

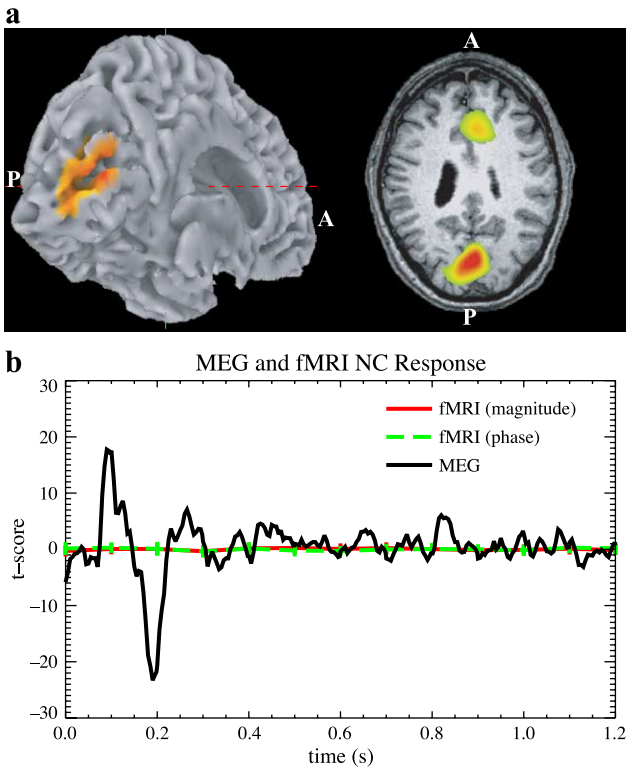

Fig. 6. Example of the MEG results as measured by the dual m-sequence method. Shown are averages of three runs on a single subject (same as Fig. 4). (a) Indication of location of MEG activity. Activated areas, as determined from SAM analysis (see text), were overlain on a surface-rendered map of left hemisphere (left) and axial oblique slice (right) of anatomical MRI data. Anterior and posterior anatomical locations are indicated with A and P, respectively. (b) Comparison of MEG and MRI sensitivity for the detection of neuronal currents. The MEG–IR (in black), obtained from a single channel, shows highly significant signals, while the average magnitude MRI IR (in red) indicates insignificant NC-related signals. The vertical (red) bars indicate the standard deviation across the BOLD-based ROI. Phase MRI IR results are shown in green.

neuronal currents. In practice, the percentage TSD is not independent of TE (e.g., in the case where thermal noise contributes significantly to the TSD), leading to an upper boundary for the optimal TE value.

The TE value of 81 ms used in the current work is similar to earlier methods, and close to the time scale of maximal neuronal current change, as measured with MEG. A potential change in current direction within the TE interval (which is possible judging from the multiphasic character of the MEG signal) might eliminate (rephase) some of the signal dephasing and reduce sensitivity. However, in our model of microscopic current changes in dendrites, this should not cancel all effects on MRI signal magnitude. The reason is that the spatial scale of the induced microscopic magnetic field gradients is on the order of the dendritic diameter (approximately 1 μm), which is smaller than the average grey matter diffusion distance during TE of at least 6 μm. Furthermore, the fact that the experiments incorporating a 50-ms delay between stimulus and data acquisition showed similar results argues against the importance of this rephasing phenomenon for microscopic effects.

Another factor that affects the absolute (in contrast to relative or percentage) NC-related signal change is the static magnetic field strength. The field strength used in the current study (3.0 T) was increased as compared to earlier studies (1.5 and 1.9 T). Although the increased magnetic field strength leads to increased T2*-related signal loss, this is to a large extent compensated for with the increased SNR available with the higher field.

For the signal change related to BOLD effects, our TE of 81 ms is longer than the optimal value at course spatial resolution (Fera et al., 2004). However, the BOLD optimum is quite broad, and the reduction in BOLD sensitivity is estimated at less than 30% (Fera et al., 2004).

(2) Apart from a low NC-related signal change, a potential reason for the failure to observe a significant NC response with MRI is a poor temporal signal stability, as expressed by the TSD. The average TSD values were 2.87% and 0.49% for single pixel and ROI-averaged magnitude signals, respectively. The value of 0.49% for the ROI-based TSD is low compared to conventional fMRI experiments. This is attributed to the high acquisition rate used in this study, which allowed elimination of cardiac and respiratory fluctuations through spectral filtering. The result is an improved sensitivity for the detection of ROI-based signal changes.

On the other hand, the single-pixel TSD was increased (i.e., inferior) compared to conventional BOLD fMRI experiments and attributed to the reduced SNR (ranging from 30 to 50) resulting from long TE and short TR used in the current study. The SNR reduction due to the short TR (100 ms), as compared with the longer TRs of 2 and 4 s used in earlier NC methods, was estimated at three- to fourfold. This SNR loss was largely offset by the use of a surface coil array, which had a sensitivity of at least threefold over a conventional birdcage coil (de Zwart et al., 2004), used in earlier studies. Nevertheless, there is clearly room for improvement with regards to the single-pixel TSD.

(3) The number of signal averages was increased by using a high stimulation rate. Since a binary m-sequence has a close to 50% duty cycle, and two binary m-sequences were used in a modulatory fashion, the overall duty cycle was about 25%. Combined with the 100-ms m-sequence base period, this resulted in an average stimulation rate of 2.5 events per second. The duty cycle could be improved to 50% by abolishing the use of the modulatory (slow) m-sequence; however, this would also eliminate the BOLD reference signal and prohibit quantitative comparison of sensitivity to BOLD and NC effects and analysis of NC effects using a BOLD-based ROI. Although previous methods used different stimuli, it appears their presentation rates were similar (Kamei et al., 1999) or much reduced (Xiong et al., 2003) compared to the current study. Preliminary results from MEG experiments that investigated the dependence of MEG signal amplitude on the stimulation rate of a flickering checkerboard (results not shown) suggest a fairly broad maximum around 10 Hz, consistent with our m-sequence base period of 100 ms.

Summarized, the discrepancy between the current study and earlier reports (Kamei et al., 1999; Xiong et al., 2003) in observing NC effects with MRI is not related to an inferior sensitivity of our method. Overall, our method achieved superior sensitivity due to increased averaging. The improvement was largest for the analyses based on ROI-averaged signals.

Separation of BOLD and NC effects

An alternative explanation for the discrepancy between the current results and earlier reports (Kamei et al., 1999; Xiong et al., 2003) is the improved suppression of BOLD contamination achieved with the m-sequence method. Suppression of BOLD signals is obtained in two stages. First, correlation with the slow m-sequence separates BOLD and NC effects in time, due to the delay of the BOLD signal relative to the NC effects. This was evident from the small (3%) remaining fraction of BOLD signal in the time segment used for extraction of the NC IR. Second, correlation with the rapid m-sequence is in effect a high-pass filter, resulting in an additional five- to tenfold suppression of the BOLD signal, as indicated by simulations. In contrast, it is unclear how much suppression of BOLD signals is achieved with the method presented by Kamei et al. (1999). The suppression is based on the assumption that BOLD signals are unaltered when the EPI read gradient is inverted. However, this might not apply to BOLD-related macroscopic phase effects, which could contaminate the NC signals. In the study by Xiong et al. (2003), suppression of BOLD signals was based on the fact that the stimulation rate (2 s) was faster than the BOLD IR, resulting in a steady state signal. However, the particular design of this experiment involving the combination of multiple time-staggered runs to extract rapid signals is prone to artifacts related to variations across runs. For example, conditions that vary (slowly) across runs, such as fatigue and attention, could manifest as rapidly changing signals and (mis)interpreted as NC effects.

Possibility of measuring neuronal currents with MRI

The results of the current study suggest that the sensitivity of MRI to detect NCs related to the visual-evoked response is too low to be practically useful using today's MRI technology and 3.0-T field strength. Although it is possible that the use of a different MRI field strength might lead to improved sensitivity, we believe it is doubtful that this improvement alone will be adequate to make NC-MRI a robust methodology. Despite the improved sensitivity of the presented method to detect NC effects and its improved suppression of BOLD contrast, earlier results suggesting the feasibility of NC-based fMRI could not be reproduced. Nevertheless, this does not necessarily mean that MRI cannot detect any of the electrical activity occurring in human brain. Other than

evoked responses, there might be electrical activity that involves larger numbers of neurons or has different characteristics that might make it more visible to MRI. For example, under certain conditions, the human brain exhibits oscillatory electrical signals in specific frequency bands. In EEG and MEG, oscillations in the 8- to 12-Hz band (alpha band) can have amplitudes that are an order of magnitude larger than somatosensory-evoked responses. They often occur during states of relaxation in the absence of visual input and can be time-locked to a stimulus (Pfurtscheller, 1992). With certain, dedicated experimental designs, it might be possible to detect such activity with MRI.

Acknowledgments

Jerzy Bodurka, Martijn Jansma, and Alan Koretsky (all at NIH) are acknowledged for helpful and stimulating discussions.

References

Bodurka, J., Bandettini, P.A., 2002. Toward direct mapping of neuronal activity: MRI detection of ultraweak, transient magnetic field changes. Magn. Reson. Med. 47, 1052–1058.

Bodurka, J., Ledden, P., van Gelderen, P., Chu, R., de Zwart, J.A., Duyn, J.H., 2004. Scalable multichannel MRI data acquisition system. Magn. Reson. Med. 51, 165–171.

Bruder, H., Fischer, H., Reinfelder, H.E., Schmitt, F., 1992. Image reconstruction for echo planar imaging with nonequidistant k-space sampling. Magn. Reson. Med. 23, 311–323.

Buracas, G.T., Boynton, G.M., 2002. Efficient design of event-related fMRI experiments using m-sequences. NeuroImage 16, 801–813.

de Zwart, J.A., Van Gelderen, P., Kellman, P., Duyn, J.H., 2002. Application of sensitivity-encoded echo-planar imaging for blood oxygen level-dependent functional brain imaging dagger. Magn. Reson. Med. 48, 1011–1020.

de Zwart, J.A., Ledden, P.J., van Gelderen, P., Bodurka, J., Chu, R., Duyn, J.H., 2004. Signal-to-noise and parallel imaging performance of a 16-channel receive-only brain coil array at 3.0 Tesla. Magn. Reson. Med. 51, 22–26.

Duyn, J.H., 1997. Steady state effects in fast gradient echo magnetic resonance imaging. Magn. Reson. Med. 37, 559–568.

Duyn, J.H., Moonen, C.T., van Yperen, G.H., de Boer, R.W., Luyten, P.R., 1994. Inflow versus deoxyhemoglobin effects in BOLD functional MRI using gradient echoes at 1.5 T. NMR Biomed. 7, 83–88.

Fera, F., Yongbi, M.N., van Gelderen, P., Frank, J.A., Mattay, V.S., Duyn, J.H., 2004. EPI–BOLD fMRI of human motor cortex at 1.5 T and 3.0 T: sensitivity dependence on echo time and acquisition bandwidth. J. Magn. Reson. Imaging 19, 19–26.

Horton, J.C., Hoyt, W.F., 1991. The representation of the visual field in human striate cortex. A revision of the classic Holmes map. Arch. Ophthalmol. 109, 816–824.

Kamei, H.I.K., Yoshikawa, K., Ueno, S., 1999. Neuronal current distribution imaging using magnetic resonance. IEEE Tans. Magn. 35, 4109–4111.

Kellman, P., Gelderen, P., de Zwart, J.A., Duyn, J.H., 2003. Method for functional MRI mapping of nonlinear response. NeuroImage 19, 190–199.

Konn, D., Gowland, P., Bowtell, R., 2003. MRI detection of weak magnetic fields due to an extended current dipole in a conducting sphere: a model for direct detection of neuronal currents in the brain. Magn. Reson. Med. 50, 40–49.

Kwong, K.K., Belliveau, J.W., Chesler, D.A., Goldberg, I.E., Weisskoff, R.M., Poncelet, B.P., Kennedy, D.N., Hoppel, B.E., Cohen, M.S., Turner, R., et al., 1992. Dynamic magnetic resonance imaging of human brain activity during primary sensory stimulation. Proc. Natl. Acad. Sci. U. S. A. 89, 5675–5679.

Lee, A.T., Glover, G.H., Meyer, C.H., 1995. Discrimination of large venous vessels in time-course spiral blood-oxygen-level-dependent magnetic-resonance functional neuroimaging. Magn. Reson. Med. 33, 745–754.

Mandeville, J.B., Marota, J.J., 1999. Vascular filters of functional MRI: spatial localization using BOLD and CBV contrast. Magn. Reson. Med. 42, 591–598.

Menon, R.S., Ogawa, S., Tank, D.W., Ugurbil, K., 1993. Tesla gradient recalled echo characteristics of photic stimulation-induced signal changes in the human primary visual cortex. Magn. Reson. Med. 30, 380–386.

Mugler III, J.P., Brookeman, J.R., 1990. Three-dimensional magnetization-prepared rapid gradient-echo imaging (3D MP RAGE). Magn. Reson. Med. 15, 152–157.

Pfurtscheller, G., 1992. Event-related synchronization (ERS): an electro-physiological correlate of cortical areas at rest. Electroencephalogr. Clin. Neurophysiol. 83, 62–69.

Robinson, S.E., Virba, J., 2002. Functional neuroimaging by synthetic aperture magnetometry. In: Yoshimoto, T., Kotani, M., Kuriki, S., Karibe, H., Nkasato, N. (Eds.), Recent Advances in Biomagnetism. Tohoku Univ. Press, Sendai, Japan, pp. 302–305.

Shoham, D., Grinvald, A., 2001. The cortical representation of the hand in macaque and human area S-I: high resolution optical imaging. J. Neurosci. 21, 6820–6835.

Sutter, E.E., 2001. Imaging visual function with the multifocal m-sequence technique. Vision Res. 41, 1241–1255.

Weisskoff, R.M., Zuo, C.S., Boxerman, J.L., Rosen, B.R., 1994. Micro-scopic susceptibility variation and transverse relaxation: theory and experiment. Magn. Reson. Med. 31, 601–610.

Xiong, J., Fox, P.T., Gao, J.H., 2003. Directly mapping magnetic field effects of neuronal activity by magnetic resonance imaging. Hum. Brain Mapp. 20, 41–49.

Yablonskiy, D.A., Haacke, E.M., 1994. Theory of NMR signal behavior in magnetically inhomogeneous tissues: the static dephasing regime. Magn. Reson. Med. 32, 749–763.

Zonta, M., Angulo, M.C., Gobbo, S., Rosengarten, B., Hossmann, K.A., Pozzan, T., Carmignoto, G., 2003. Neuron-to-astrocyte signaling is central to the dynamic control of brain microcirculation. Nat. Neurosci. 6, 43–50.